

Structure and Dynamics of the Hydrogen-Bond Network around (*R,R*)-Pterocarpan with Biological Activity in Aqueous Solution

Giuliano Alagona,* Caterina Ghio, and Susanna Monti

CNR–IPCF, Institute for Physical Chemistry Processes, Molecular Modeling Laboratory, Via Moruzzi 1, I-56124 Pisa, Italy

Received: May 23, 2005; In Final Form: June 24, 2005

Molecular dynamics simulations were carried out in the presence of 2380 water molecules (TIP3P) to explore the conformational preferences of 3,9-dimethoxy-4-prenylpterocarpan (bitucarpin A) and 3,9-dihydroxy-4,8-diprenylpterocarpan (erybraedin C) and the H-bond network around them, using the empirical general AMBER force field (GAFF). Specific angle and torsional parameters have been improved in order to match the geometries of the minimum energy structures obtained from an earlier DFT/ab initio study in vacuo, taking into account a few configurations [Alagona, G.; Ghio, C.; Monti, S. *Phys. Chem. Chem. Phys.* **2004**, 6, 2849–2857]. RESP partial charges were assigned to reproduce the electrostatic potential determined at the HF/6-31G* level of theory. The analysis of trajectories allowed the conformations of bitucarpin and erybraedin as well as the distribution of water molecules around them to be elucidated. During one of the simulations only, the scaffold of erybraedin undergoes interconversion from its most stable H_t conformation to the O_t one and vice versa. Radial distribution functions, coordination numbers, and angular distributions put forward the extent of solvent structure and the hydrogen bonding behavior of their various (methoxy, hydroxyl, or ethereal) oxygen atoms. The distribution of solvent molecules in the first and second solvation shells as well as the residence times for the different solute–solvent interacting sites have been considered.

I. Introduction

Pterocarpan are stress-induced metabolite constituents, acting as protective agents¹ (phytoalexins), of plants of the genus *Psoralea* (Figure 1) common in the Mediterranean area and widely spread also in other regions of our planet, such as North and South America, the southern part of Africa, and Australia. Because of their biological activity, long-recognized, they are widely used in traditional medicine as antibacterial, antifungal and antiinflammatory agents.² Most of them possess antimicrobial, insecticidal, oestrogenic, and cytotoxic activities, while natural or synthetic products have been shown to have high antiviral as well as anti-HIV activities.³

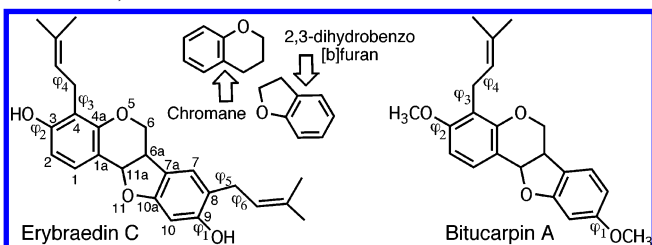
The main structural feature of pterocarpan is the simultaneous presence in their skeleton of two fused chromophores, producing two chiral centers (6a and 11a; see Chart 1). The most common substituents to the pterocarpan backbone are prenyl chains and hydroxy/methoxy groups, whose chemical properties and location significantly affect their activity. In an earlier investigation all the possible skeleton and side-chain arrangements of 3,9-dihydroxy-pterocarpan and 3,9-dimethoxy-4-prenylpterocarpan (bitucarpin A) have been studied in vacuo at the B3LYP/6-31G* level.⁴ Reference is made to that study as far as configurations, helicity, stabilities, and conformer names or interconversion pathways are concerned. For 3,9-dihydroxy-4,8-diprenylpterocarpan (erybraedin C), only the outward–outward OH group arrangement, consistent with the methoxy one, had been considered in that study, to keep the conformational minima of the prenyl side chains analogous to those found in bitucarpin A. A thorough examination of all the



Figure 1. Specimen (flowers and leaves) of *Psoralea bituminosa*, popularly indicated in Italy as “Trifoglio cavallino” (horse clover).

* Corresponding author. Phone: +39-050-3152450. Fax: +39-050-3152442. E-mail: G.Alagona@ipcf.cnr.it.

CHART 1: Structures, Rotatable Bonds, and Atom Numbering of Bitucarpin A and Erybraedin C (H and OX Groups Are Numbered after the C Atom They Are Linked to)^a



^a The constituting chromophores (chromane and 2,3-dihydrobenzo[b]furan), once fused, produce two chiral centers (6a and 11a) in the pterocarpan backbone.

possible erybraedin C conformations in vacuo has been carried out still at the B3LYP/6-31G* level in a subsequent study.⁵

Nonetheless, to obtain a deeper insight into the conformational properties of these compounds, they need to be studied in aqueous solution, because the presence of the solvent may affect the side chain/backbone conformations and/or the relative stabilities of the various forms. Furthermore, the knowledge of the hydration shell surrounding a biologically active molecule can shed some light on its mode of action, still unknown. Concerning pterocarpan, distinct hypotheses have been put forward according to which biological activity one is interested in: their anticancer activity might involve ternary complexes with topoisomerase and DNA, while binding to Cu^{2+} these compounds might prevent its oxidizing action.

The present study is thus devoted to the analysis of molecular dynamics simulations in water, with validation of relevant force field parameters, to elucidate the hydrophilic and hydrophobic regions of these compounds and possible persisting interactions to be included in cluster solvation models.

II. Systems Considered

Beside the backbone arrangements, named H_t and O_t depending on which atom is trans with respect to H_{6a} , and the (6a, 11a) chirality, the structures of the two pterocarpan under investigation are characterized by the side chain orientations, determined by the φ_1 ($\text{C}_{10}\text{C}_9\text{OX}$) and φ_2 ($\text{C}_2\text{C}_3\text{OX}$) with $\text{X} = \text{methyl (Me) or H}$, φ_3 ($\text{C}_3\text{C}_4\text{CC}$), φ_4 (C_4CCC), φ_5 ($\text{C}_9\text{C}_8\text{CC}$), and φ_6 (C_8CCC) dihedral angles, the latter two where applicable, as shown in Chart 1. Since the *cis* (6aR, 11aR) configurations, that furthermore correspond to the natural compound,⁶ turned out to be about 10 kcal/mol lower in energy than the *trans* (6aR, 11aS) configuration, the *cis* configuration has been considered throughout this investigation. As far as the O_t conformers are concerned, they resulted about 2 kcal/mol higher in energy than the H_t ones. Therefore the starting conformations were taken H_t ; when not otherwise specified, along the simulations they maintained their H_t arrangement.

A. Bitucarpin. The main starting conformation for bitucarpin A, shown in Figure 2, with $\varphi_3 = -81.4^\circ$ and $\varphi_4 = -114.1^\circ$, is the lowest energy structure obtained in vacuo at the B3LYP/6-31G* level in a previous study.⁴ Three additional minima (with $\varphi_3/\varphi_4 = -96.9^\circ/114.3^\circ$, $94.9^\circ/-115.0^\circ$, and $82.1^\circ/115.9^\circ$, respectively) with analogous stability were obtained. A small barrier of ~ 1.5 kcal/mol separated the minima with φ_4 values of $\pm 120^\circ$, whereas a barrier of ~ 5 kcal/mol had been found between the opposite perpendicular arrangements ($\varphi_3 \approx \pm 90^\circ$).

B. Erybraedin. Two main starting conformations among those obtained in vacuo for erybraedin C have been used for

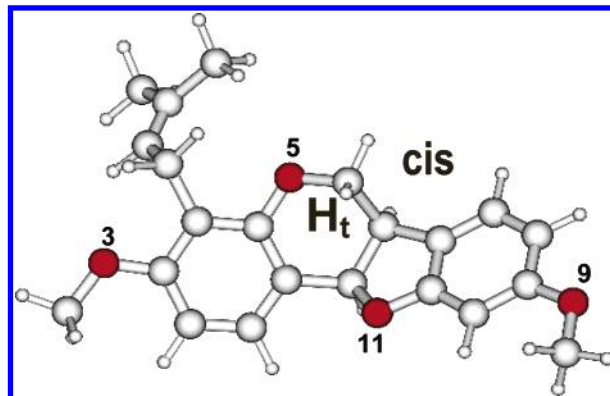


Figure 2. B3LYP/6-31G* lowest energy structure for bitucarpin A in vacuo. The O_t structure (i.e., with O_5 trans with respect to the hydrogen at C_{6a}) is about 2 kcal/mol higher in energy than H_t .

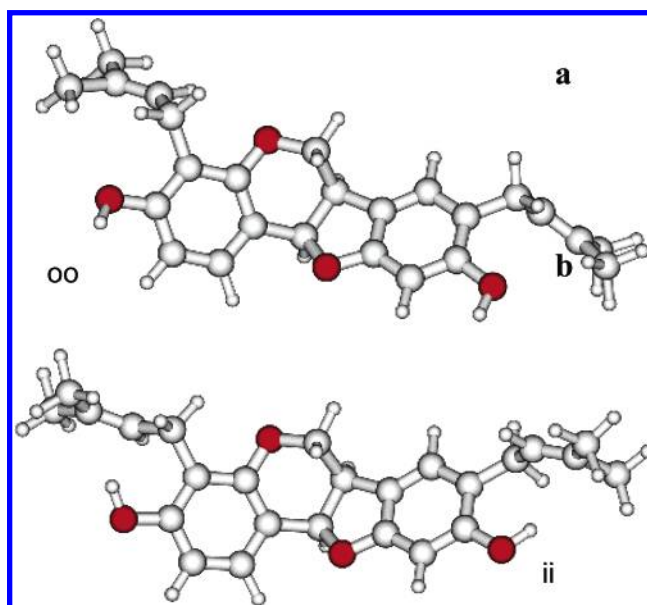


Figure 3. B3LYP/6-31G* structures for erybraedin C used as starting arrangements. The ii structure, with the hydroxy hydrogens pointing toward the π density of the prenyl double bonds, is among the lowest energy ones in vacuo.

the molecular dynamics (MD) simulations in solution. They differ primarily because of the spatial disposition of the hydroxy groups, thus for the φ_1 ($\text{C}_{10}\text{C}_9\text{OH}$) and φ_2 ($\text{C}_2\text{C}_3\text{OH}$) values, and for the prenyl side chain orientation, determined by the φ_3/φ_4 and φ_5/φ_6 couples of torsions. In the structure displayed in Figure 3a, both hydroxy hydrogens point outward ($\varphi_1 \approx \varphi_2 \approx 0^\circ$);⁴ it is therefore named oo for short in what follows. In the other structure considered (Figure 3b), named ii, both hydroxy hydrogens point inward and face the prenyl side chains ($\varphi_1 \approx \varphi_2 \approx 180^\circ$). This is the most stable arrangement in vacuo at the B3LYP/6-31G* level,⁵ the oo conformation being 4.2 kcal/mol higher in energy.

The $\varphi_3, \varphi_4/\varphi_5, \varphi_6$ prenyl torsional angles for oo are -97.9° , $113.9^\circ/+81.5^\circ, -118.5^\circ$, respectively, with both prenyl side chains pointing away from the observer of Figure 3. For ii the prenyl dihedrals measure $+52.1^\circ, -132.9^\circ/+56.8^\circ, -132.3^\circ$ in the order displayed above. It is noteworthy, however, that in the case of ii the prenyl side chain at C_4 (on the left-hand side in Figure 3b) is still below the ring plane, whereas the prenyl side chain at C_8 (on the right-hand side in Figure 3b) is above the ring plane. The relevant backbone arrangements are well-conserved in both cases.

III. Computational Details

Molecular dynamics simulations were carried out with the AMBER7 software^{7a} to explore the conformational preferences of bitucarpin A and erybraedin C in water solution. MD simulations were based on the GAFF,^{7b} whose parameters cover most of the organic chemistry space. It was however necessary to improve specific torsional parameters in order to match the geometries of the minimum energy structures obtained in vacuo during our earlier density functional theory (DFT) conformational search,⁴ especially as far as the prenyl side chain arrangements are concerned. The newly derived parameters (reported in Table S1 of the Supporting Information, SI) were actually able to reproduce the dihedral angles defining the position of prenyl side chains, taking into account at the same time, in the case of erybraedin, the interactions of the hydroxy groups with the prenylic π system.

MD simulations were performed and the long-range electrostatic interactions were treated via the particle-mesh Ewald (PME) method.⁸ The dielectric constant, ϵ , was set to 1 and the TIP3P model⁹ was employed for the explicit representation of 2380 water molecules. All MD simulations were performed using periodic boundary conditions in the NPT ensemble at constant pressure (1 atm) and at temperatures maintained at 298 K by coupling the system to a thermal bath with Berendsen's algorithm.¹⁰ Bitucarpin and erybraedin partial charges (reported in Tables S2 and S3 of SI) were assigned to reproduce the molecular electrostatic potential determined at the HF/6-31G* level of theory¹¹ according to the RESP methodology.¹² The lowest energy geometries (cis, 6aR, 11aR) from earlier DFT calculations were chosen as starting structures and inserted in the simulation box. Other structures used as starting point for additional simulations, carried out for comparison, are described where appropriate.

The integration time step was set to 1 fs, and the X–H stretching modes were frozen with the SHAKE algorithm.¹³ After 2000 steps of energy minimization, the system was heated under constant-volume conditions to 500 K over 5 ps of dynamics while keeping fixed the solute coordinates, and then cooled to 298 K over 10 ps in order to randomize water molecule positions. This first step was followed by a 25 ps equilibration at constant pressure. Starting from the equilibrated system, 1 ns production dynamics was carried out in the NPT ensemble. Configurations were stored every 0.1 ps for further analysis. One of the reviewers requested an additional nanosecond of dynamics for oo erybraedin. For the sake of comparison, also the dynamics of ii erybraedin has been resumed for the same period of time.

IV. Molecular Dynamics Analysis

The analysis of the trajectories was performed by examining the structural parameters, distinguishing the conformations of bitucarpin and erybraedin, and the distribution of water molecules around the two compounds. The distributions of dihedral angles, defining the orientation of the two methoxy or hydroxy groups, respectively, and the orientation of the prenyl side chain(s), have been recorded. To obtain information about the extent of solvent structure and to illustrate the hydrogen bonding behavior of bitucarpin and erybraedin oxygen atoms, intermolecular radial distribution functions (RDFs) $O_x \cdots H_w$ and the corresponding coordination numbers (CN) were calculated. The RDFs describe the local density of the solvent at a distance r from the solute atoms relative to the bulk density and approach unity for large distances where the local density converges to

its bulk value. The angular distributions of water hydrogens within 3 Å of the solute oxygens have also been recorded.

The distribution of the solvent molecules in the first and second solvation shells and the residence times for the different solute–solvent interaction sites are reported. Residence times correspond to the length of time that a solvent molecule remains in a site before moving to another site. They are important to discriminate between labile and persistent water molecules. Mean residence times (MRTs) of water molecules around solute oxygen atoms were calculated considering only those solvent molecules within a distance of 3 Å of any solute oxygen. Any water that returned to this coordination shell after escaping for a time period shorter than 1 ps has been considered to be continuously bound to the examined solute oxygen whereas any molecule that was out of this coordination shell for longer than 1 ps was considered to be a free molecule. The mean residence times of 0, 1, and 2 solvent molecules around each oxygen atom of the solute are also reported.

A. Conformational Properties. The conformations obtained in solution starting from the lowest energy structure in vacuo for bitucarpin A, shown in Figure 2, are described in terms of the torsion angle distributions defining the methoxy group spatial disposition and the prenyl side chain orientation. The population distributions visited by the φ_1 ($C_{10}C_9OMe$) and φ_2 (C_2C_3OMe) torsion angles are displayed in Figure 4.

The whole angular range of -180 to $+180^\circ$ is explored in the case of φ_1 , although the prominent angular domains correspond to in-plane values around 0° and $\pm 180^\circ$. In contrast, the φ_2 values are distributed around a unique orientation (0°) with a vanishingly small tail about $\pm 90^\circ$, because of the steric hindrance of the prenyl side chain for other values of φ_2 .

The individual distribution of φ_3 (C_3C_4CC), the plain histogram in Figure 5, shows a very narrow and tall peak centered at -90° , depending of course on the starting conformation [an analogous distribution has been obtained at $+90^\circ$, starting from the other perpendicular conformer with $\varphi_3 \approx 90^\circ$], whereas the φ_4 (C_4CCC) dihedral angle, shown in Figure 5 with a diagonal pattern, exhibits a wide population around 180° with shoulders at $\pm 120^\circ$. The φ_3 and φ_4 dihedral angles are arranged as $-90^\circ/\pm 180^\circ$ pairs. This is a quite different distribution with respect to the in vacuo situation, where φ_4 values of $\pm 120^\circ$, although separated by a small barrier, were obtained for each nearly perpendicular arrangement of φ_3 . This fact indicates that extended conformations of the prenyl side chain are favored in aqueous solution. This kind of arrangement should permit a better contact of water with the O_3 and O_5 oxygens, otherwise considerably shielded in turn by the bulky side chain.

As far as erybraedin C is concerned, the φ_1 and φ_2 distributions for the simulation starting from the oo structure are shown in Figure 6. The most populated values are distributed around 0° with vanishingly small population already at $\pm 60^\circ$. The largest populations are located in the angular range -30° up to $+30^\circ$, whereas orientations around $+180^\circ$ (within $-150^\circ/+150^\circ$) are also represented (although they have almost negligible abundances), indicating that the hydroxy group, in contrast to the methoxy one, can span the whole conformational space.

The individual distribution of φ_3 , plotted in Figure 7a together with that of φ_4 , shows a marked peak centered at -90° as expected because of the starting conformation. Actually, as in the case of bitucarpin, a prenyl side chain cannot surmount the barrier (by ~ 5 kcal/mol in vacuo at the B3LYP/6-31G* level⁴), corresponding to its in-plane arrangement. The φ_4 dihedral angle distribution, also shown in Figure 7a, presents a wide spreading

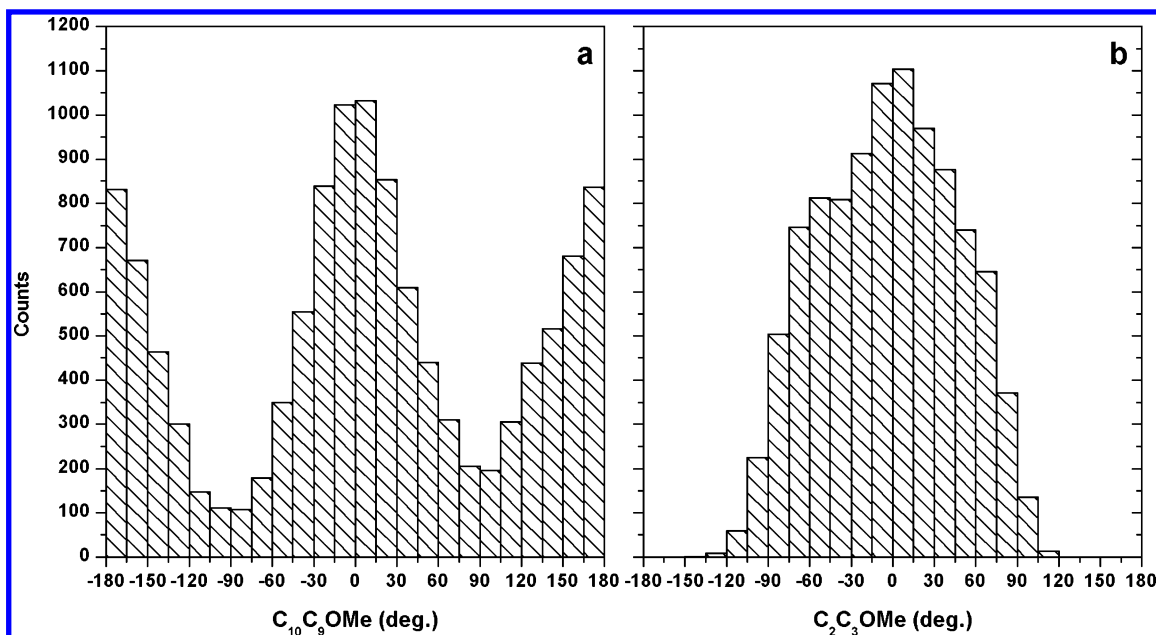


Figure 4. Counts of solvated structures of bitucarpin A with the given value of (a) φ_1 and (b) φ_2 .

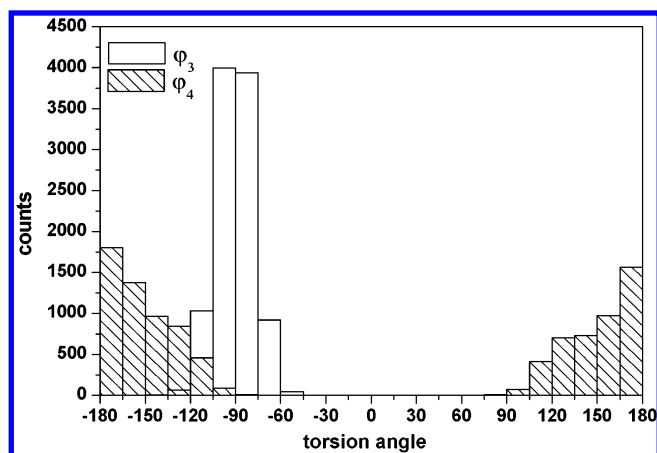


Figure 5. Counts of solvated structures of bitucarpin A with the given values of φ_3 and φ_4 (see legend).

over a large range of values (-90° to $+90^\circ$) about its maximum around $+180^\circ$. Therefore, similarly to bitucarpin A, φ_3 and φ_4 are arranged mostly as -90° , $\pm 180^\circ$ pairs, because the small barrier, which separates in vacuo the $\varphi_4 \approx \pm 120^\circ$ conformers, disappears in solution, favoring an extended conformation of the prenyl side chains.

Analogous distributions are obtained for φ_5 and φ_6 both plotted in Figure 7b. As already stated for φ_3 , φ_5 cannot surmount the barrier corresponding to its in-plane arrangement and change its sign: rather, only a limited fluctuation about its starting value ($\approx +81^\circ$, as stated in section II) is found. Therefore the behavior of the prenyl side chains is conserved and hardly affected by the nearby groups.

The distributions of φ_3 , φ_4 , φ_5 , and φ_6 for the simulation starting from the ii conformer of erybraedin are fairly similar to those reported in Figure 7b, even though the initial values of φ_3 and φ_5 were about 52° and 57° , respectively, with the hydroxy hydrogens pointing toward the prenyl double bonds. The presence of the solvent, however, disrupts those preferential interactions, making the torsion angle distributions analogous to those recorded for the simulation starting from the oo rotamer. Thus, the φ_3 and φ_5 distributions remain in the positive half-plane, centered about $+90^\circ$: the hydroxy hydrogen in water no longer interacts with the double-bond π distribution, because

of the presence of water oxygens that are much stronger H-bond acceptors than π electrons.

To clarify the slightly different behavior of the φ_1 and φ_2 distributions, despite the starting orientations opposite in ii with respect to oo, also the φ_1 and φ_2 distributions for the ii simulation are shown in Figure 8 (for a pictorial view with the four distributions superimposed, see Figure S1 in SI).

It is apparent that φ_2 behaves almost exactly in the same way in both cases, whereas φ_1 frequently visits arrangements close to the starting one. This ability is possibly due to the loosely bound waters in the vicinity of the nearby prenyl side chain (at C₈). On the contrary, the water molecules interacting with O₅ prevent the prenyl side chain at C₄ to move far from the OH group for a sufficiently long period of time.

The PME algorithm,¹⁴ sometimes charged of reducing the conformational sampling capability of MD simulations although mainly for ionic solutions,¹⁵ seemingly does not affect the present simulations of neutral systems.

B. Radial Distribution Functions, θ Distributions, and Coordination Numbers. A remarkable difference between the radial distribution functions for O₁₁...H_w and O₉...H_w, on one hand, and for O₅...H_w and O₃...H_w, on the other hand, can be noticed in Figure 9a, where the RDFs for bitucarpin are displayed. The RDFs for O₁₁...H_w and O₉...H_w show a first peak centered at approximately 1.99 and 2.05 Å, respectively, which can be considered evidence of the formation of stable hydrogen bonds between the water hydrogens and the O₁₁ and O₉ atoms of the solute. In contrast, both O₅...H_w and O₃...H_w RDFs do not display any first peak at short intermolecular distances but a shoulder of very low amplitude at about 2.20 Å, which is more pronounced in the O₃...H_w RDF. This suggests that the O₅ and O₃ atoms can form weak and much longer transient hydrogen bonds to the solvent, because of the wagging prenyl side chain. Taking, in default of a clear minimum, 2.65 Å as the coordination radius, coordination numbers of 0.6 are obtained for both oxygens. The coordination numbers derived from the O₁₁...H_w and O₉...H_w RDFs are equal to 1.0 and 0.8, respectively, thus indicating that both oxygen atoms are involved in one intermolecular hydrogen bond with water, on the average, as expected due to their less hindered positions. Much broader peaks located at intermediate distances in the O₅...H_w and O₃...

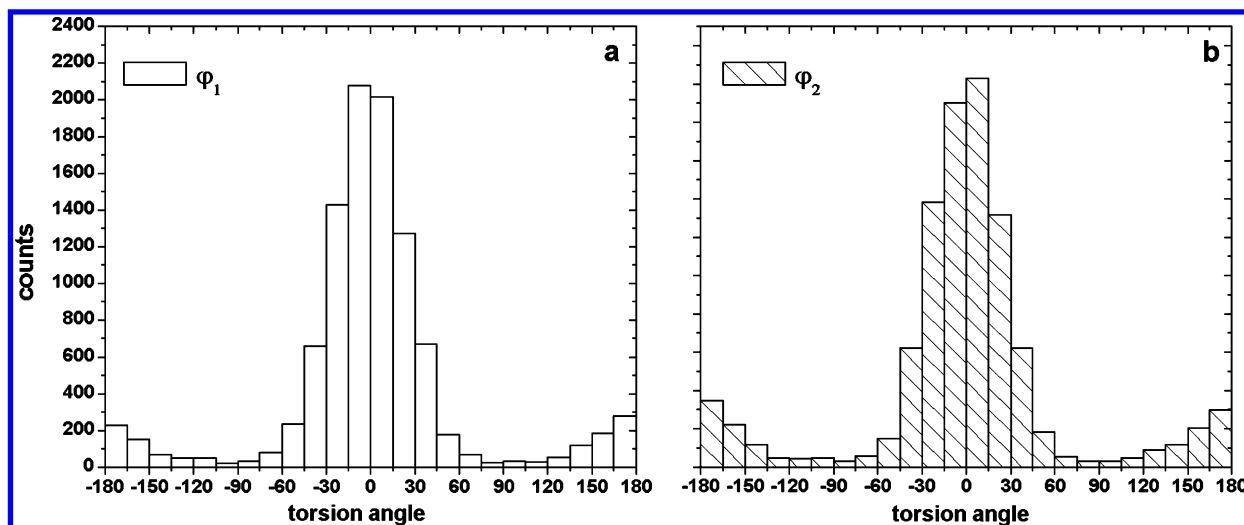


Figure 6. Counts of solvated structures of erybraedin C (oo starting conformation) with the given values of (a) ϕ_1 (C₁₀C₉OH) and (b) ϕ_2 (C₂C₃-OH).

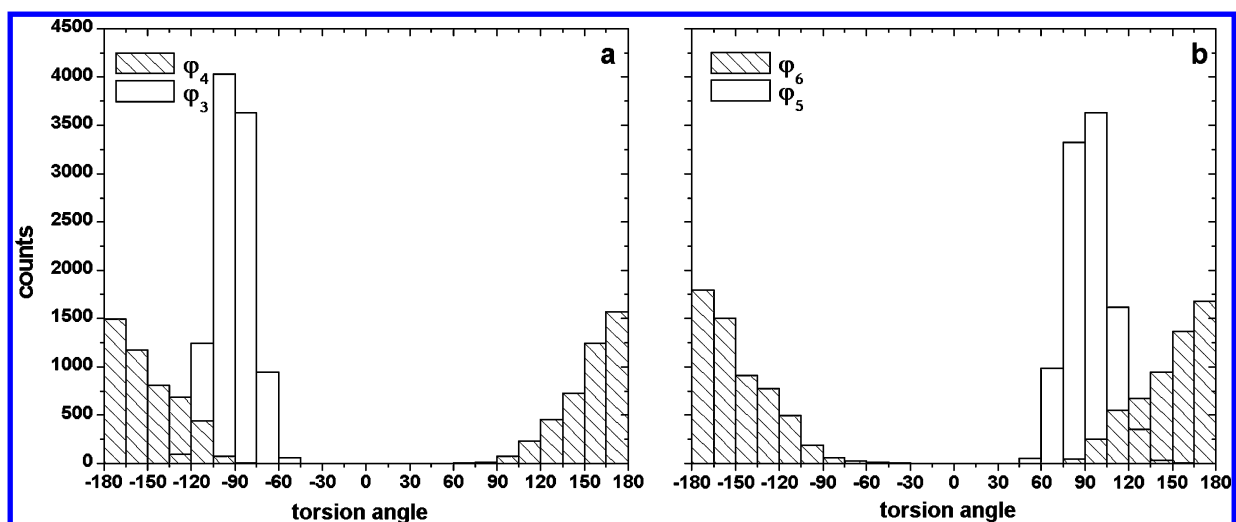


Figure 7. Counts of solvated structures of erybraedin C (oo starting conformation) with the given values of (a) ϕ_3 (C₃C₄CC, plain histogram) and ϕ_4 (C₄CCC, filled histogram) and (b) ϕ_5 (C₉C₈CC, plain histogram) and ϕ_6 (C₈CCC, filled histogram).

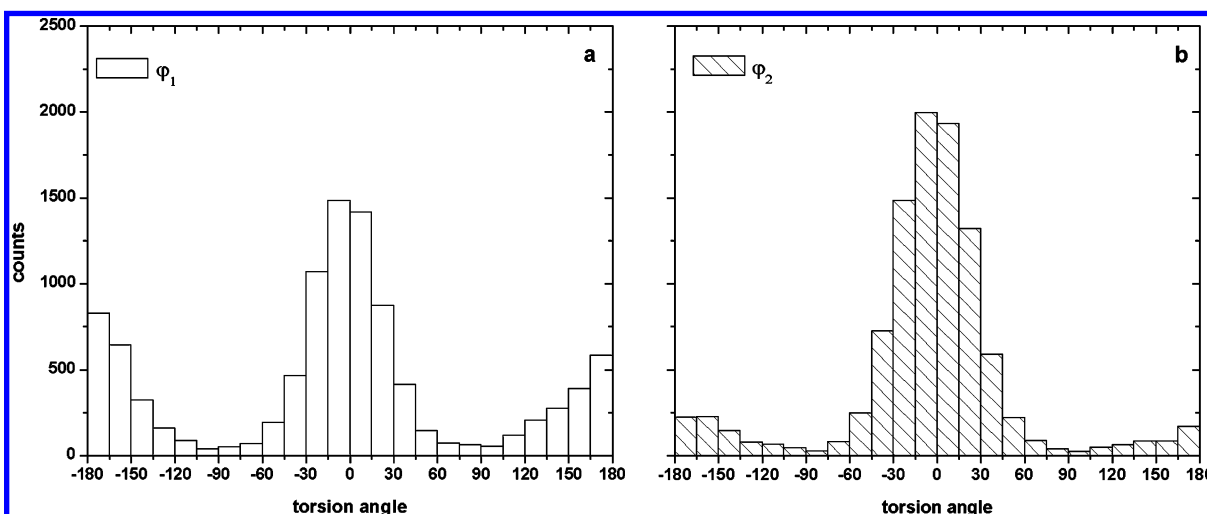


Figure 8. Counts of solvated structures of erybraedin C (ii starting conformation) with the given values of (a) ϕ_1 (C₁₀C₉OH) and (b) ϕ_2 (C₂C₃OH).

\cdots H_w RDFs indicate on the other hand that the ordered shell of water is slightly less well-defined, because O₅ and O₃, essentially less available for hydrogen bonding, see the water molecules bound to the other polar sites nearby.

In the case of the simulation starting from oo erybraedin, the

O₃ \cdots H_w, O₉ \cdots H_w, and O₁₁ \cdots H_w RDFs, displayed in Figure 9b, show a first peak for the first solvation shell with a maximum at about 2.0 Å, a minimum at about 2.5 Å, and a coordination number of 1.0, values that are typical for hydrogen bonds. Indeed, during the MD simulation the hydroxyl groups and the

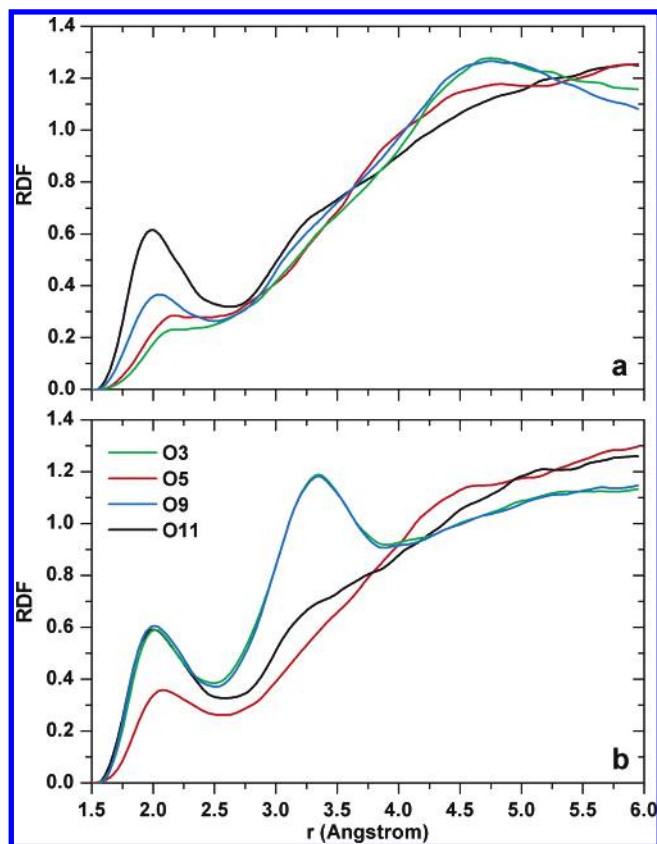


Figure 9. Radial distribution functions $O_3 \cdots H_w$ (green), $O_5 \cdots H_w$ (red), $O_9 \cdots H_w$ (blue), and $O_{11} \cdots H_w$ (black) of water hydrogens around the oxygens of (a) bitucarpin A and (b) oo erybraedin C.

O_{11} oxygen have a high tendency to form stable and strong hydrogen bonds with water molecules. A closer inspection of the $O_3 \cdots H_w$, $O_9 \cdots H_w$, and $O_{11} \cdots H_w$ RDFs reveals that while the amplitude of the first maximum is identical for all of them, the amplitude associated with the first minimum for $O_{11} \cdots H_w$ is lower than for the $O_3(O_9) \cdots H_w$ RDF. This feature can be interpreted as evidence of a more structured H-bond network around O_3 and O_9 , indicating that O_3 and O_9 are more tightly hydrogen bonded to water than O_{11} . In contrast, the $O_5 \cdots H_w$ RDF shows a broader and weaker peak at about 2.1 Å with a coordination number of 0.7, suggesting that the O_5 oxygen is poorly solvated by water. The $O_3 \cdots H_w$ and $O_9 \cdots H_w$ RDFs displayed also a second peak for the second solvation shell at about 3.4 Å with a coordination number of 9.

To evaluate the orientation of the water molecules in the first hydration shell of both solutes, the distribution of the θ angle, which is the angle between the water H and the outer (positive) part of the axis joining the two oxygens, a farther 3 Å at most, as shown in Chart 2 in a general case, has been examined.

It is apparent from Figure 10a that, for bitucarpin A, where only etheral oxygens (i.e. H-bond acceptor) are present, there are two main peaks, about 75 and 175°, related to H-bond donor waters, with one of their Hs roughly pointing toward the polar group in the solute. Interestingly, this distribution is slightly flatter for O_5 and O_3 because of the vicinity of the prenyl side chain, whereas water orientations around O_9 and O_{11} are less perturbed.

In the case of the first shell of hydration around erybraedin in the simulation starting from its oo structure, water arrangements are remarkably different between etheral and hydroxy oxygens, as can be derived from Figure 10b. While the θ angle distributions of etheral oxygens are fairly consistent with those

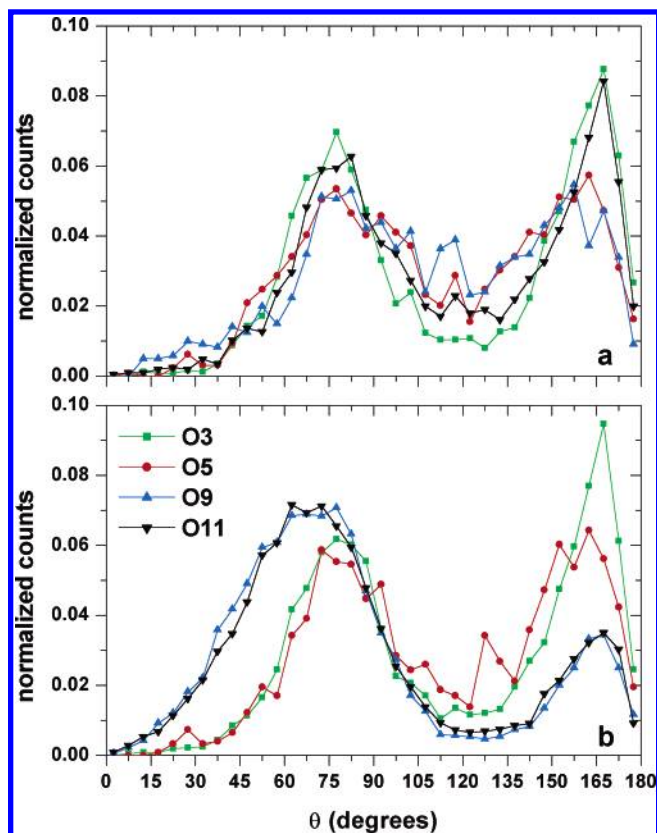
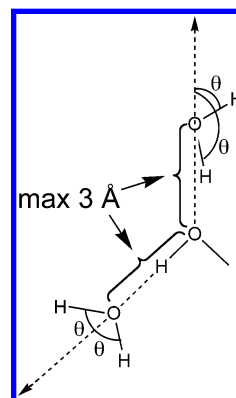


Figure 10. θ angle distributions of water hydrogens within 3 Å (see Chart 2) of the various oxygens O_3 (blue), O_5 (red), O_9 (black), and O_{11} (green) of (a) bitucarpin A and (b) oo erybraedin C.

CHART 2: Definition of the θ Angle with Respect to H-Bond Acceptor and Donor Sites



of bitucarpin, the double character of the hydroxy group, behaving analogously to water both as H-bond donors and H-bond acceptors, comes out clearly from the distributions about O_3 and O_9 . Those distributions are much wider by about 60°, because the hydrogens of waters behave as H-bond acceptors and add themselves to the other hydrogen of those pointing toward the hydroxy oxygen, whose number however decreases with respect to bitucarpin. This trend of the θ angle distributions (not shown) is conserved also in the simulation starting from ii erybraedin. To avoid duplicated discussions, the analysis is carried out for the oo erybraedin simulation, because of the structure interconversion occurred within the solute (see below). Only remarkable differences between the simulations are pointed out.

A distinctive feature of the simulation starting from oo erybraedin is that the $O_5C_6C_{6a}H_{6a}$ dihedral, defining the helicity of the six-membered heteroring, which usually spans the interval

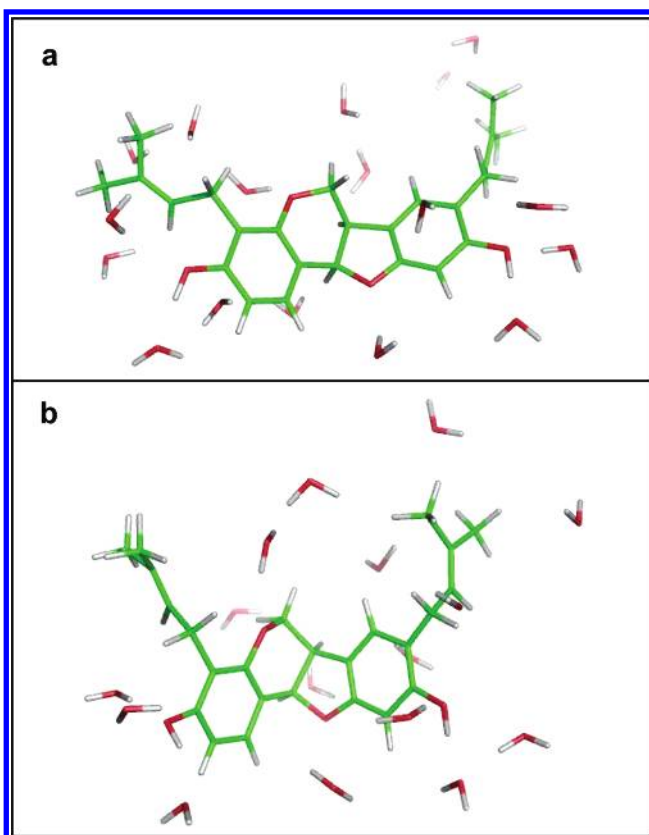


Figure 11. Two snapshots along the simulation starting from the oo arrangement. Only the water molecules within 2.5 Å of any of the solute atoms are displayed: (a) 500 ps frame (17 H₂O) and (b) 1 ns frame (16 H₂O). Depth cueing is used to reduce the brilliance of locations farther from the observer.

60–90°, after about 0.82 ns jumps to a transoid arrangement, spanning the interval 150–180° most of the time (see Figure S2 of SI). The structures taken in the 0.4 ps occurring for the interconversion are displayed in Figure S3a of SI. After about 0.5 ns the structure reverts to its previous arrangement in 0.2 ps (see Figure S3b in SI) without jumping back to O_t in the subsequent period of time. Therefore, the H_t structure (Figure 11a) seemingly is capable of interconversion to the O_t one during the simulation (Figure 11b). No interconversion at all is observed however during 2 ns of simulation time starting from ii erybraedin. Since for 3,9-dihydroxypterocarpan at the B3LYP/6-31G* level, computed earlier,⁴ the O_t structure is higher in energy by about 2 kcal/mol than the H_t one and the barrier heights to interconversion are 6.3 and 6.8 kcal/mol, respectively, as already recalled, the stabilities of the various conformers of 3,9-dihydroxy-pterocarpan have been computed using AMBER/GAFF on the B3LYP/6-31G* structures. The H_t structure turns out to be more stable than the O_t one by only 0.5 kcal/mol (0.6 kcal/mol after geometry optimization with AMBER, possible only for local minima), while the barriers are 1 and 3.9 kcal/mol, respectively. Nonetheless, even with investigation of bitucarpin and erybraedin themselves at the B3LYP/6-31G* level, the shape of the potential energy surface does not change.⁵ Therefore it is likely that the force field underestimates the energy gaps. On the other hand, the occurrence of O_t in one case and for a very short segment of dynamics is in fair agreement with experimental results, suggesting that the equilibrium is shifted in favor of H_t.¹⁶

C. Mean Residence Times. The large availability to solvent interaction of O₁₁ and O₉ in bitucarpin A is evident from the water mean residence times, while O₃ and O₅ are somewhat

TABLE 1: Mean Residence Times (ps) for a Particular Number of Waters around Each Oxygen in Bitucarpin A

atom	0 water	1 water	2 waters
O ₃	8.6	63.3	
O ₅	8.0	26.9	
O ₉		77.9	26.5
O ₁₁		23.7	17.3

TABLE 2: Mean Residence Times (ps) for a Particular Number of Waters around Each Oxygen in Erybraedin C

atom	0 water	1 water	2 waters	3 waters	4 waters
O ₃			136.4	95.2	73.9
O ₅	6.8	64.5			
O ₉		56.8	104.0	53.1	
O ₁₁		24.0	14.7		

hindered due to the bulky prenyl chain in the vicinity, as can be derived by examining the data reported in Table 1. However, even O₃ and O₅ are almost always surrounded by at least one water molecule: in fact, the 0-water MRTs for both of them are lower than 10 ps. The 1-water MRTs for O₉ and O₃ are the longest ones; nevertheless the O₉ atom is more exposed to the solvent than O₃ and thus easily accessible to water molecules that exchange extensively between the first and the second solvation shell. Waters at O₁₁ and O₅ have mean residence times lower than 30 ps; the main difference between them, however, consists of the fact that around O₁₁ there is a frequent alternation between one and two water molecules, while in the case of O₅ only one water molecule moves in and out of the first coordination shell.

The mean residence times for the simulation starting from the oo structure of erybraedin are reported in Table 2. Longer mean residence times have been found for the hydroxy oxygens (O₃ and O₉). O₉ is always surrounded by at least one water molecule, whereas for O₃ the minimum number of water molecules is equal to two. Besides knowing the duration of waters in specific sites, it is interesting to understand how they move around. The most interesting information is not the trajectory of individual water molecules but the flow of water between sites. Indeed, the presence of nonzero (i.e. 1, 2, 3, 4) water mean residence times indicates an intense motion of solvent molecules between the coordination shells of the O₃ and O₉ atoms, confirming the higher availability of the hydroxy groups, which are at the same time H-bond donors and acceptors, to interact favorably with the solvent. At the other end of the time scale, waters near O₁₁ and O₅ have MRTs lower than 65 ps. O₅ has less water neighbors than O₁₁, as expected because it is actually more buried than O₁₁, and one water molecule only moves back and forth between the first and the second hydration shell. Consequently, O₁₁, being more exposed to the solvent than O₅, exchanges one or two neighboring waters.

As far as water positions are concerned, it can be helpful to take a look at a few snapshots along a simulation. Although devoid of any statistical significance, those snapshots might give a better insight into the water arrangements about the solute. As an example two frames at 500 and 1000 ps of a simulation are displayed in Figure 11 (only water molecules within 2.5 Å at most of any solute atom are shown). The water positions in the first hydration shell are actually consistent with the radial distribution function and residence time pictures. In Figure 11a, there is a water hydrogen (H_w) at 2.41 Å from O₃, 2.30 Å from O₅, and 2.04 Å from O₁₁. Two H_w belonging to different water molecules are H-bonded to O₉ (with H_w...O₉ separations of 2.02 and 2.22 Å, respectively), while distinct O_w are H-bonded to H₉ (i.e. the H at O₉) and H₃, (O_w...H_n = 1.60 and 2.02 Å,

respectively). A water molecule is roughly pointing one of its Hs to a C=C double bond: its distance from each C atom is 2.51 and 2.60 Å, respectively. In Figure 11b, where the solute structure is O_t, there are three water molecules at O₃ (two as proton donors with H_w...O₃ = 2.01 and 2.44 Å, respectively; one as a proton acceptor with O_w...H₃ = 2.05 Å), while there are just two water molecules at O₉ (H_w...O₉ = 1.99 Å and O_w...H₉ = 1.80 Å; the latter along the other lone-pair has an H-bonding water which is very close to the solute). Single water molecules are H-bonded to O₅ and O₁₁ (H_w...O_n = 2.04 and 2.49 Å, respectively). A few water molecules are located around the prenyl groups as observed also in Figure 11a.

This solvation picture can be exploited to extract a proper set of structures for subsequent cluster calculations embedded in a continuum.¹⁷ It is actually difficult to obtain water clusters from ab initio or DFT calculations,¹⁸ because in general water molecules prefer to H-bond to each other, thus producing a guess of a second solvation shell without completing the first one.

V. Conclusions

The wealth of attractive biological activities of pterocarpan prompted us to explore the conformational features of bitucarpin A and erybraedin C in aqueous solution, making use of molecular dynamics simulations with GAFF. Few specific bond and torsion angles have been tuned in order to reproduce the prenyl side chain arrangements obtained in earlier DFT calculations. The purpose of this investigation is 2-fold: (i) to estimate the preferred conformations in solution of their scaffold/typical side chains and (ii) to characterize the best H-bond acceptor and donor anchor points as well as lipophilic binding sites in order to describe eventually the possible pharmacophore by inference, validating at the same time the force field parameters.

The analysis of the dihedral angle distributions suggests that in aqueous solution both the methoxy and hydroxy groups point toward the solvent. A predominance of the values about 0° is in fact observed, although a noticeable distribution of torsions about 180° has been found at O₉, mainly for bitucarpin, due to the missing prenyl side chain nearby. The steric hindrance of the bulky group sharply affects the erybraedin C₂C₃OH and C₁₀C₉OH distributions even for the simulation starting from the ii structure, whose C₁₀C₉OH distribution however shows a memory of its starting value.

The prenyl side chains remain in their original arrangement below (or above) the heteroring plane and assume an elongated conformation. A distinctive difference with respect to the in vacuo structure of the prenyl side chains is their extended posture (with C_nCC=C close to +180°, whereas values close to ±130° had been obtained in vacuo at the B3LYP/6-31G* level).

The radial distribution functions display a different behavior between bitucarpin and erybraedin, primarily due to the absence of hydroxy groups in bitucarpin, that behave as proton donors besides as proton acceptors. This behavior is put forward also in the θ angle distributions of water hydrogens within 3 Å of any of the solute oxygens [θ is defined as the angle between H_w and the outer part of the axis joining O_w and a solute O (see Chart 2)]. In bitucarpin, the solvent exposition of O₉ and O₁₁, larger than that of O₃ and O₅, somewhat hindered by the bulky chain between them, comes out clearly from the mean residence times. The solvent exposition information for erybraedin confirms the high solvent availability of hydroxy groups, whereas O₅ turns out to be much more buried than O₁₁.

A number of water molecules are found in the C=C regions of the prenyl groups, with one of their hydrogen atoms pointing toward the double-bond π density. Seemingly this effect is properly accounted for in the GAFF force field.

Supporting Information Available: Comparison of the φ₁ and φ₂ dihedral angle distribution in the simulations starting from ii and oo erybraedin C (Figure S1), flip angle distribution along 2 ns of the oo erybraedin C dynamics (Figure S2), H_t to O_t and O_t to H_t interconversions along the erybraedin C oo dynamics (Figure S3), modified force field parameters (Table S1), and PDB files with HF/6-31G* RESP charges for bitucarpin A and erybraedin C, with atom numbering (Tables S2 and S3, respectively). This material is available free of charge via the Internet at <http://pubs.acs.org>.

References and Notes

- (1) (a) Kuc, J. *Annu. Rev. Phytopathol.* **1972**, *10*, 207. (b) Dewick, P. M.; Steel, M. J. *Phytochemistry* **1982**, *21*, 1599.
- (2) (a) Latha, P. G.; Evans, D. A.; Panikkar, K. R.; Jayavardhanan, K. K. *Fitoterapia* **2000**, *71*, 223. (b) Bandara, B. M.; Kumar, N. S.; Samaranyake, K. M. *J. Ethnopharmacol.* **1989**, *25*, 73.
- (3) (a) Sato, M.; Tanaka, H.; Fujiwara, S.; Hirata, M.; Yamaguchi, R.; Etoh, H.; Tokuda, C. *Phytomedicine* **2003**, *10*, 427. (b) Seo, E. K.; Kim, N. C.; Mi, Q.; Chai, H.; Wani, M. E.; Navarro, H. A.; Burgess, J. P.; Graham, J. G.; Cabieses, F.; Tan, G. T.; Farnsworth, N. R.; Pezzuto, J. M.; Kinghorn, A. D. *J. Nat. Prod.* **2001**, *64*, 1483. (c) McKee, T. C.; Bokesch, H. R.; McCormick, J. L.; Rashid, M. A.; Spielvogel, D.; Gustafson, K. R.; Alavanja, M. M.; Cardelline, J. H. II; Boyd, M. R. *J. Nat. Prod.* **1997**, *60*, 431.
- (4) Alagona, G.; Ghio, C.; Monti, S. *Phys. Chem. Chem. Phys.* **2004**, *6*, 2849.
- (5) Alagona, G.; Ghio, C. Manuscript in preparation.
- (6) Pachler, K. G. R.; Underwood, W. G. E. *Tetrahedron* **1967**, *23*, 1817.
- (7) (a) Case, D. A.; Pearlman, D. A.; Caldwell, J. W.; Cheatham, T. E., III; Wang, J.; Ross, W. S.; Simmerling, C. L.; Darden, T. A.; Merz, K. M.; Stanton, R. V.; Cheng, A. L.; Vincent, J. J.; Crouley, M.; Tsui, V.; Gohlke, H.; Radmer, R. J.; Duan, Y.; Pitera, J.; Massova, I.; Seibel, G. L.; Singh, U. C.; Weiner, P. K.; Kollman, P. A. *AMBER 7*; University of California: San Francisco, 2002. (b) Wang, J.; Wolf, R. M.; Caldwell, J. W.; Kollman, P. A.; Case, D. A. *J. Comput. Chem.* **2004**, *25*, 1157.
- (8) (a) Darden, T.; York, D.; Pedersen, L. J. *Chem. Phys.* **1993**, *98*, 10089. (b) Essmann, U.; Perera, L.; Berkowitz, M. L.; Darden, T.; Lee, H.; Pedersen, L. G. *J. Chem. Phys.* **1995**, *101*, 8577.
- (9) Jorgensen, W. L. *J. Am. Chem. Soc.* **1981**, *103*, 335.
- (10) Berendsen, H. J. C.; Postma, J. P. M.; vanGunsteren, W. F.; DiNola, A.; Haak, J. R. *J. Comput. Phys.* **1984**, *81*, 3684.
- (11) Hehre, W. J.; Radom, L.; Schleyer, P. v. R.; Pople, J. A. *Ab Initio Molecular Orbital Theory*; Wiley: New York, 1986.
- (12) (a) Cieplak, P.; Cornell, W. D.; Bayly, C. I.; Kollman, P. A. *J. Comput. Chem.* **1995**, *16*, 1357. (b) Bayly, C. I.; Cieplak, P.; Cornell, W. D.; Kollman, P. A. *J. Phys. Chem.* **1993**, *97*, 10269.
- (13) Ryckaert, J. P.; Ciccotti, G.; Berendsen, H. J. J. *J. Comput. Phys.* **1977**, *23*, 327.
- (14) Other authors support PME because of its attractive feature of keeping the starting conformations stable during dynamics: (a) Cheatham, T. E.; Miller, J. L.; Fox, T.; Darden, T. A.; Kollman, P. A. *J. Am. Chem. Soc.* **1995**, *117*, 4193. (b) Simmerling, C.; Lee, M. R.; Ortiz, A. R.; Kolinski, A.; Skolnick, J.; Kollman, P. A. *J. Am. Chem. Soc.* **2000**, *122*, 8392.
- (15) (a) Hünenberger, P. H.; McCammon, J. A. *Biophys. Chem.* **1999**, *78*, 69. (b) Kastenholz, M. A.; Hünenberger, P. H. *J. Phys. Chem. B* **2004**, *108*, 774, and references therein.
- (16) Pachler, K. G. R.; Underwood, W. G. E. *Tetrahedron* **1967**, *23*, 1817.
- (17) (a) Alagona, G.; Ghio, C.; Monti, S. *Int. J. Quantum Chem.* **2002**, *88*, 133. (b) Mennucci, B.; Martínez, J. M. *J. Phys. Chem. B* **2005**, *109*, 9818.
- (18) Sensible structures can be obtained either in 1:1 clusters¹⁹ or when a single water molecule per hydration site (being the hydration sites enough far away from each other) is considered.
- (19) (a) Alagona, G.; Ghio, C. *Int. J. Quantum Chem.* **2002**, *90*, 641. (b) Nagy, P. I.; Alagona, G.; Ghio, C.; Takács-Novák, K. *J. Am. Chem. Soc.* **2003**, *125*, 2770.